GROWTH MECHANISMS DURING THIN FILM CRYSTALLIZATION FROM THE MELT

Loren Pfeiffer, A. E. Gelman, K. A. Jackson, and K. W. West*

AT&T Bell Laboratories
Murray Hill, New Jersey 07974

ABSTRACT

We develop a model that appears to account for the existence of a new mode of crystallization recently discovered during zone-melt-recrystallization (ZMR) of silicon thin films on SiO_2 using a scanned strip heater or lamp. Transition to the new crystallization regime is induced by reducing the temperature of the scanned upper heater strip, thus reducing dT/dy, the thermal gradient along the direction of scan at the silicon solidification front. If dT/dy $\leqslant 4^\circ$ K/mm, the single crystal films have long non-branched subboundaries with tilt misalignments of 0.1° or less, a lateral separation in excess of 50 μm, and consist of rows of short dislocations threading through the film thickness and terminating at the two SiO_2 layers. This is in marked contrast to material ZMR scanned at higher dT/dy which shows conventionally branched 1° to 3° subboundaries that consist of edge dislocations running in the plane of the film often for several hundred microns.

Our model extends the {111} faceted-freezing-front picture we have developed previously to take into account the freezing profile with respect to film thickness, and in particular to such profiles at the intersections of pairs of {111} facets where subboundaries are known to form. We propose that the melt-freezing interface profiles at these interior corner intersections are aligned approximately normal to the scan in the high gradient case, but become tilted towards the plane of the SiO_2 cap layer for the low gradient case. This tilting accounts in a natural way for the transition from in-plane to threading dislocations.

Networks of low angle grain boundaries or subboundaries are the singular characteristic crystallographic defect[1,2] found in thin film silicon zone-melt-recrystallized (ZMR) on vitreous SiO_2 substrates. Essentially all of the recent work in ZMR of Silicon-on-Insulator (SOI) is aimed at eliminating subboundaries or in mitigating their effects. Recently in our laboratory and elsewhere large areas of subboundary-free thin film ZMR SOI have been obtained.[3–6] It is now clear that this subboundary-free material is due to a new type of recrystallization that is qualitatively different from the conventional ZMR seen using lasers, lamps and strip heaters over the past decade and longer. In this paper we will (i) demonstrate the truth of this claim, (ii) show that control of the thermal gradient near the freezing front is the key to accessing the new crystallization regime, and (iii) propose a physical model that ascribes the differences in the two recrystallization regimes to differences in the geometry of the liquid-freezing interface during growth.

Figure 1 is a scanning electron micrograph at two magnifications of conventional high thermal gradient ZMR silicon-on-insulator material in electron backscatter channeling contrast. The individual subgrains are shaded in varying tones of gray depending on the textural alignment of each subgrain with respect to

* Present address: Dept. of Statistics, Harvard University, Cambridge, MA 02138

Mat. Res. Soc. Symp. Proc. Vol. 74. ©1987 Materials Research Society

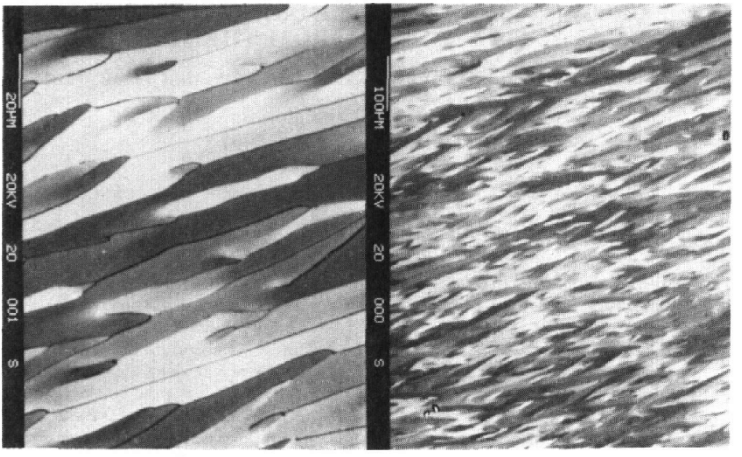

1. Scanning Electron Micrograph in electron backscatter channeling contrast showing two magnifications in the same area of a conventional high-gradient ZMR SOI sample.

the electron beam axis. On the basis of electron channeling pattern[5] analysis we know that no subgrain is misaligned by more than $\sim 2^{\circ}$ from the average Si(100) texture. This is the origin of the striking pseudo-periodic white-to-gray ripple effect seen in the low magnification micrograph on the right. The maximum crystallographic deviation from Si(100) occurs on the scale of a few subgrains; there is no evidence for cumulative effects which would result in textural drift on a larger scale.

The figure is representative of the best ZMR thin film SOI obtainable using conventional high gradient scanning. On the other hand, the low thermal gradient material referred to above is more than an order of magnitude better in textural alignment, with no area deviating by as much as 0.1° from the average Si(100) texture.[5] Thus grain-to-grain variations of the low gradient material become almost imperceptible in electron backscatter mode at the same level of gray scale contrast.[3]

The most convincing demonstration of the *qualitative* difference between the low and high gradient material is, however, revealed by transmission electron micrographs of the individual dislocations that collectively form the subboundaries in the two cases. Subboundaries in the high-gradient material (top planview micrograph of Fig. 2) typically consist of many long edge dislocations running parallel to one another in the plane of the film for hundreds of microns.[2] Subboundaries in the low thermal gradient material are very different. The bottom planview micrograph of Fig. 2 shows that they typically consist of many short dislocations that thread reasonably directly through the thickness of the silicon film terminating on the two encapsulating oxide layers.

We now take up the issue of how one experimentally accesses this new low gradient mode of crystallization. Operationally as indicated above one simply reduces the power to the scanning upper strip heater which reduces the width of

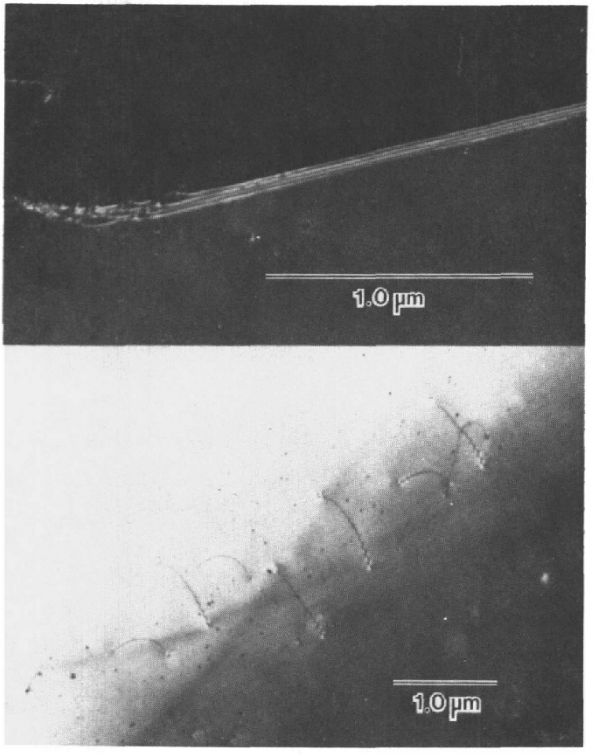

2. Planview Transmission Electron Micrographs of SOI subboundaries. Top photo is a high-gradient subboundary showing dislocations running in the plane of the Si film. Bottom photo is a low-gradient subboundary showing rows of threading dislocations.

the traveling melt zone to near zero. There are, however, two additional requirements. First, the scan velocity must be reduced to ~ 0.5 mm/sec or less. If this is not done the very narrow molten zone, whose temperature is just at the silicon melting point (see thermal analysis below) does not have sufficient time to completely melt all the polycrystalline feedstock, so the ZMR results in large grain polysilicon. We note this effect misled us for a time into the belief that very slow scans were required for proper low-gradient crystallization. Very slow scan velocities are not required provided the polycrystalline silicon completely melts during the ZMR.

We also find that the transition to the low-gradient regime is more reliably induced if the silicon film thickness is at least 1 μm rather than 0.5 μm or less. This is believed to be due to a related requirement that the top of the silicon thin film be hotter than the bottom at the solidification interface, so as to properly bias the selection of interfacial facets on the growing solid. We discuss this point below in connection with our physical model of low gradient recrystallization.

We now digress briefly to discuss a thermal analysis of our scanned wire geometry, as this will allow us to be more quantitative about what is meant by low or high thermal gradients. We use the geometry of Fig. 3 with a hot scanning wire and a 0.5 mm thick silicon substrate wafer heated from below to ~ 1475 K in the regions far from the upper wire. The SOI structure is divided into a finite grid of unequal rectangular cells each containing only a single material. The wafer extent is assumed to indefinitely large, the wire indefinitely long, and a coordinate system is chosen that moves with the scanning wire. The heat flow between the cells is obtained by solving the differential equation for heat flow iteratively by standard methods.[7]

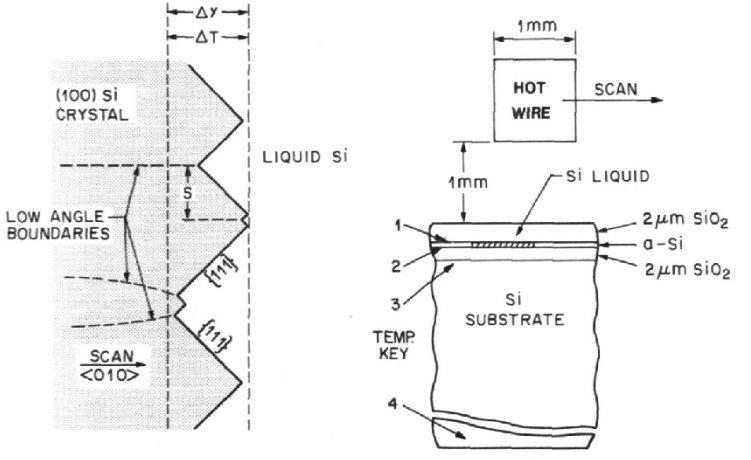

3. Schematic drawings showing the geometry the facets in plan view, and the SOI structure. The numbers keyed in the structure cross section at the right refer to surfaces at which the temperature is plotted in the profiles of Figs. 4 and 5.

The results are profiles as in Figs. 4 and 5 which establish the relation between the local temperature of the film, T, and the distance y from the wire. Figure 4 is a typical high gradient profile. The silicon film thickness is 1 μm, the wire-to-wafer spacing is 0.5 mm, the scan velocity is 0.5 mm/sec, and the upper wire is sufficiently hot to create a 0.75 mm wide melt zone, which at its center is seen to be 4 K above the Si melting point. The profile of Fig. 5 is calculated for identical conditions except the temperature of the scanning wire is reduced until the width of the scanning molten zone has shrunk to 0.27 mm. The maximum temperature is again near the center of the melt zone, but now is only 0.4 K above the silicon melting point. This profile for which dT/dy at the trailing recrystallization front is 4 mm/ K is a low-gradient case, as can be seen in the example of defect-etched SOI material obtained under these conditions. The pointers mark the subboundary lines which are either missing entirely or evident only as isolated rows of dislocations or dislocation clusters. The contrast between this film and the defect etched sample done under high gradient conditions in Fig. 4 is evident.

From these calculated profiles it is clear why low thermal gradients are often

correlated with narrow melt zones and low melt temperatures. It is also evident that a wider wire spaced more closely to the SOI wafer would be useful in obtaining low gradient material. With these principles we find we can achieve low gradient crystallization at will on 1 μm or thicker silicon films across entire 100 mm dia. wafers.

In the remainder of this paper we propose a model for these effects. The model invokes postulated differences in the melt-crystallization interface geometry to account for the properties of the low and high gradient SOI crystal growth regimes. Our starting point is the {111} faceted interface model developed by ourselves[8] and the MIT-Lincoln group[9] to account for the characteristic branched patterns formed by high-gradient ZMR subboundaries in silicon thin films. As we intend to build on that picture we will review briefly some of its important properties recast to aid visualizing the solidification front in three dimensions.

Strip heater ZMR Si films on SiO_2 are experimentally found to be (100) textured, and because <010> Si is a fast growth direction,[10] this is also typically

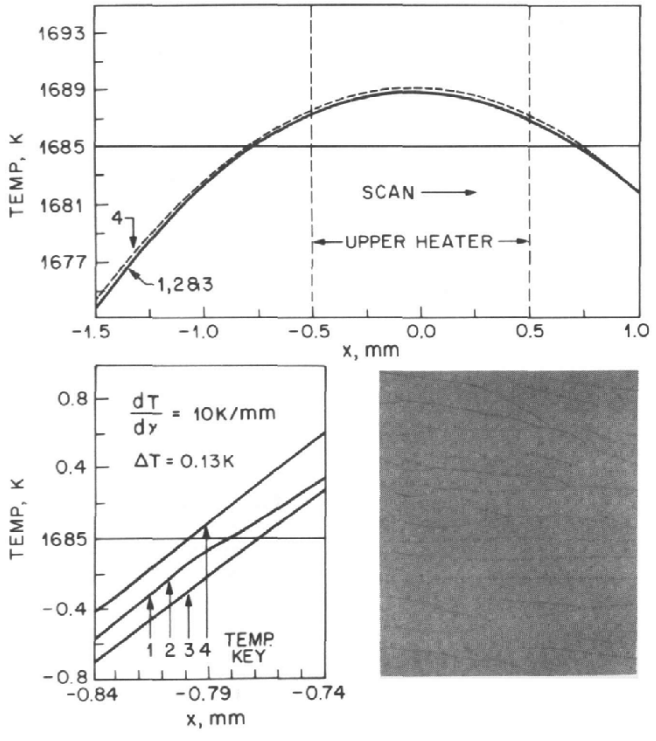

4. Profiles, for the high-gradient case of the SOI film temperature as a function of distance from the scanning wire, as calculated from a finite element differential heat flow analysis. The microphoto is a defect etched SOI film run under these conditions. The numbers 1 through 4 refer to temperatures calculated at the surfaces keyed in Fig. 3.

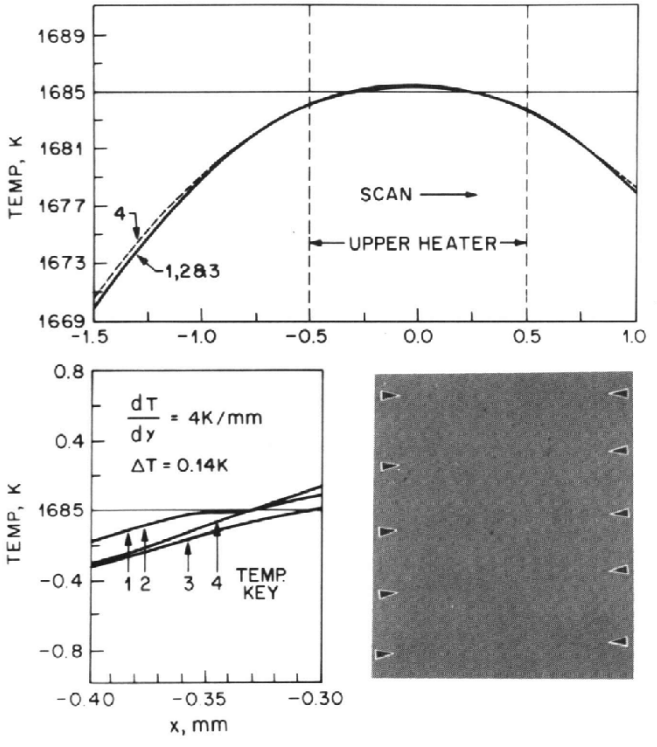

5. Profiles for the low-gradient case, of the SOI film temperature as a function of distance from the scanning wire, as calculated from a finite element differential heat flow analysis. The microphoto is a defect etched SOI film run under these conditions. The numbers 1 through 4 refer to temperatures calculated at the surfaces keyed in Fig. 3.

the growth axis which is aligned in the direction of scan. The interface between the melt and the Si crystal is assumed to be everywhere terminated on the Si {111} crystal planes as <111> is the slowest growth direction,[10] and the growth on these planes is assumed to be nucleation limited. The subboundaries formed during ZMR are by experiment found in the solid at the interior corners formed by adjacent pairs of interfacial facets. These assumptions taken together give the planview facet geometry shown at the left of Fig. 3, and with the analysis of Ref. 10, make it possible to generate the time development of the facets, and thus plot the loci of the interior corners during faceted growth. The success of that model is the close correspondence that was found between these interior corner loci and the patterns formed by experimental subboundaries in ZMR silicon thin films.[8]

The reader may be thinking that this correspondence is nice, but is there any *direct* evidence for the existence of a faceted growth front during ZMR? The affirmative answer is provided by Fig. 6, which shows SOI films recrystallized using our strip heater modified so that the temperature of the upper heater wire could be

pulsed at 19 Hz. This method which is similar to that of Geis et al.,[9] produced a crystallization front which advanced and retreated in an oscillatory manner as the scan proceeded. These oscillations had the effect of defining the instantaneous growth front as shown in the figure. We highlighted the front in several places in the figure to guide the eye, and also performed a KOH etch pit analysis[1] to determine the crystallography of the Si film. We note that the sides of the square KOH etch pits are indeed parallel to the individual facets of the fosilized growth interface exactly as expected for {111} growth facets.

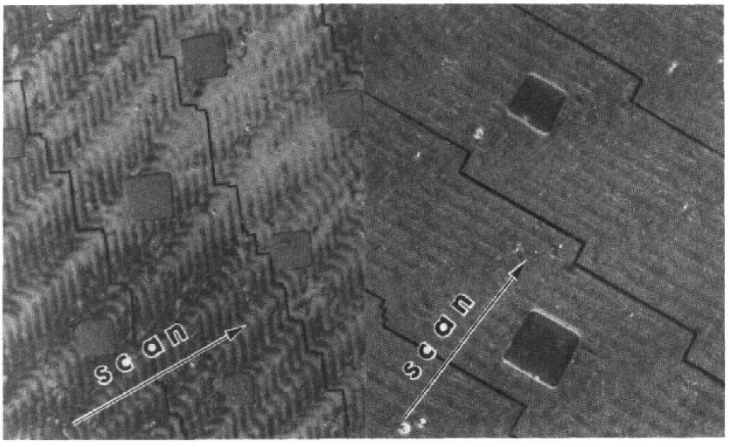

6. Direct evidence of a {111} faceted recrystallization front. SOI films recrystallized using a melt that is temperature pulsed at 19 Hz during the 0.1 mm/sec scan. The oriented squares are due to a KOH etch pit analysis, which shows that the Si film is a (100) crystal with its {111} planes parallel to the fosilized growth facets.

To make further progress we now consider this faceted melt-crystallization interface in all three dimensions. It establishes itself on some set of Si {111} planes lying between the isothermal surfaces determined by the Si melting point and the temperature of maximum undercooling of the melt appropriate to the scan velocity. For (100) textured growth in the <010> direction any combination of the planes (111), (11$\bar{1}$), ($\bar{1}$11) or ($\bar{1}$1$\bar{1}$) are possible facets for the growth front. Two possible examples of faceted growth interfaces are illustrated in Fig. 7 in three views. The lower example in each view consists of only (111) and (11$\bar{1}$) facets; it is a simple upward-tilting snowplow shape with the lower silicon film surface crystallizing always ahead of that nearest the cap surface. This is also true for the (111), (11$\bar{1}$) facet intersections. Profiles at both the exterior and interior corners as viewed from the solid extend forward at the bottom of the silicon film as compared to the top. On the other hand for the upper example in Fig. 7, the ($\bar{1}$11) facet tilts downward, and the (11$\bar{1}$) facet upward. So for this case the facet intersections at both exterior and interior corners have vertical profiles when viewed along the scanning meltwire.

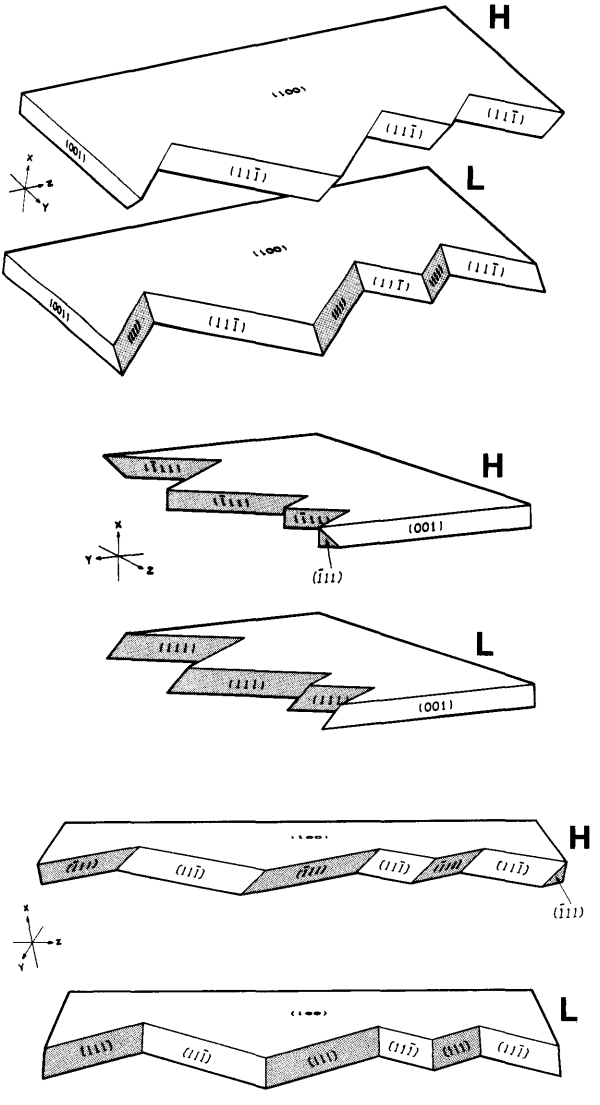

7. Examples of possible {111} faceted growth interfaces in three views. The text argues that the high thermal gradient ZMR condition selects facet structures of the type labeled H, and the low gradient condition selects type L structures.

The actual faceted interface could consist of pure examples as illustrated or complex mixtures of these cases and their mirror reflections containing also (111) facets. To get some guidance on how the faceted structure might be chosen in a given experiment, let us turn to another result obtained from the finite element thermal analysis.

Figure 8 shows the 1685°K silicon melting isotherm calculated from this analysis in the various SOI layers for both the high and low-gradient cases of Figs. 4 and 5. Observe that the isotherm is nearly vertical in the 1 μm silicon film with the high-gradient, but for the low-gradient it is slanted toward the plane of the cap oxide indicating that the silicon film is ~ .005°K hotter at the top than at its bottom surface. When these calculated contours of constant temperature for the two cases are compared with the faceted configurations of Fig. 7, it suggests that high-gradient melt conditions should favor a facet geometry of the type $(\bar{1}11)$, $(11\bar{1})$ because their vertical intersection profile most closely matches the near vertical high-gradient isotherm. Similarly, the low-gradient condition would be expected to favor facet pairs of the type (111), $(11\bar{1})$, because both the isotherm and the profiles at the facet intersections are biased so that the bottom of the film crystallizes slightly ahead of the top. Note also that this tendency to bottom leading bias would be expected to be larger for thicker Si films, just as experiment demonstrates.

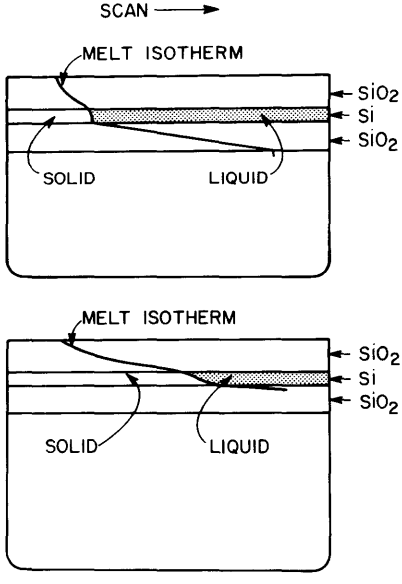

8. Isotherm profiles in a 1 μm Si film for both high and low-gradient conditions, calculated using the finite element differential heat flow analysis. The high-gradient case is at the top; the low-gradient case is at the bottom of the figure.

Our arguments thus far can be summarized by assigning facet structures of the type (111), (11$\bar{1}$) labeled L in Fig. 7 to the low-gradient experiments, and structures of the type ($\bar{1}$11), ($\bar{1}$1$\bar{1}$) (or (111), (1$\bar{1}$1)) labeled H to the high-gradient experiments. We will now attempt to relate these facet structures to differences in the recrystallized SOI material.

We concentrate on the interior corner profiles formed by the intersections of adjacent {111} facets, because it is well established[1,4] that subboundary formation occurs there. In the context of our model we have shown that the profile is vertical for high-gradient ZMR, and tilted so the bottom of the silicon film solidifies first for low-gradient ZMR. These interior corner profiles are schematically summarized in Fig. 9 for ZMR growth moving towards the right at three instants. The liquid Si melt is symbolized by shading, and any possible impurity buildup in the melt due to rejection by the growing solid is symbolized by darker shading.

Consider now dislocation formation resulting from differential thermal stresses or impurity and particulate incorporation, and suppose these stresses can be relieved by a given formation rate for dislocations as the ZMR scan proceeds. These dislocations can propagate in the growing solid *only* by extending into the new material formed at the melt-solid interface. Studies in the literature show that dislocation propagation in a growing crystal tends to be favored in directions running approximately normal to the melt-solid interface.[11] Thus for the vertical recrystallization profile of high-gradient material, each new dislocation can propagate indefinitely in the horizontal plane of the Si film. As new dislocations are continually added to those already present, sizable cumulative crystallographic distortions are built up as the subboundary is extended along the scan. However,

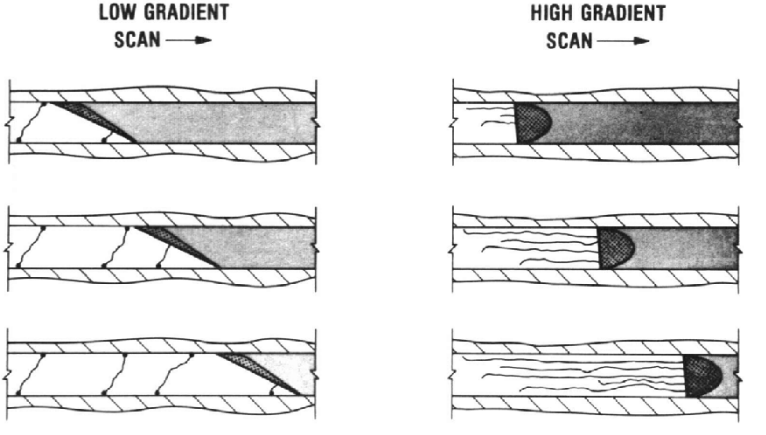

9. Cross sections showing the melt-solid profiles at the interior corners formed by the proposed facet configurations for the low and high-gradient ZMR conditions. The figure also illustrates the proposed mechanism whereby high gradient in-plane dislocations are transformed to threading dislocations as the thermal gradient is reduced below 4 K/mm.

for the slanted profile of the low-gradient material at the left in Fig. 9, the same rule of dislocation propagation normal to the melt-solid interface, results in short threading dislocations which start at the bottom of the Si film and self-terminate at the cap oxide. This accounts both for the observed transition to threading dislocations, and because cumulative effects are prevented, for the markedly better crystallographic texture found in the low-gradient films.

The authors wish to acknowledge J. M. Gibson, D. C. Joy, and G. H. Gilmer, for helpful discussions. Figures 1 and 2 are due to D. C. Joy and J. M. Gibson respectively, and are taken from collaborative work published elsewhere.

REFERENCES

[1] M. W. Geis, H. I. Smith, B-Y. Tsaur, J. C. C. Fan, D. J. Silversmith, and R. W. Mountain, J. Electrochem. Soc. *129*, 2812-18 (1982).

[2] H. Baumgart and F. Phillipp, Mat. Res. Soc. Symp. Proc. *35*, 593-8 (1985).

[3] Loren Pfeiffer, K. W. West, Scott Paine, and D. C. Joy, Mat. Res. Soc. Symp. Proc. *35*, 583-592 (1985).

[4] M. W. Geis, C. K. Chen, H. I. Smith, R. W. Mountain and L. C. Doherty, Mat. Res. Soc. Symp. Proc. *35*, 575-583 (1985).

[5] Loren Pfeiffer, K. W. West, D. C. Joy, J. M. Gibson, and A. E. Gelman, Mat. Res. Soc. Symp. Proc. *53*, 29-38 (1986).

[6] M. W. Geis, C. K. Chen, H. I. Smith, P. M. Nitishin, B-Y. Tsaur, and R. W. Mountain, Mat. Res. Soc. Symp. Proc. *53*, 39-44 (1986).

[7] A. E. Gelman, Loren Pfeiffer, G. H. Gilmer, K. A. Jackson, and K. W. West, to be published.

[8] Loren Pfeiffer, Scott Paine, G. H. Gilmer, Wim van Saarloos, and K. W. West, Phys. Rev. Letts. *54*, 1944-7 (1985).

[9] M. W. Geiss, H. I. Smith, D. J. Silversmith, R. W. Mountain, and C. V. Thompson, J. Electrochem. Soc. *130*, 1178-83 (1983).

[10] G. H. Gilmer, Mat. Res. Soc. Symp. Proc. *13*, 249 (1983).

[11] W. C. Dash, J. Appl. Phys.*30*, 459 (1959), and B. Chalmers, Principles of Solidification, John Wiley and Sons, Inc., New York, 1964 p. 307.